Paper:

Thermal Error Minimization of a Turning-Milling Center with Respect to its Multi-Functionality

Martin Mareš†, Otakar Horejš, and Jan Hornych

Research Center of Manufacturing Technology (RCMT), Department of Production Machines and Equipment,
Faculty of Mechanical Engineering, Czech Technical University in Prague (CTU)
Horská 3, 128 00 Prague 2, Czech Republic
†Corresponding author, E-mail: m.mares@rcmt.cvut.cz

[Received October 25, 2019; accepted December 11, 2019]

Achieving high workpiece accuracy is a long-term goal of machine tool designers. Many causes can explain workpiece inaccuracy, with thermal errors being the most dominant. Indirect compensation (using predictive models) is a promising thermal error reduction strategy that does not increase machine tool costs. A modeling approach using transfer functions (i.e., a dynamic method with a physical basis) has the potential to deal with this issue. The method does not require any intervention into the machine tool structure, uses a minimum of additional gauges, and its modeling and calculation speed are suitable for real-time applications that result in as much as 80% thermal error reduction. Compensation models for machine tool thermal errors using transfer functions have been successfully applied to various kinds of single-purpose machines (milling, turning, floor-type, etc.) and have been implemented directly into their control systems. The aim of this research is to describe modern trends in machine tool usage and focuses on the applicability of the modeling approach to describe the multi-functionality of a turning-milling center. A turning-milling center is capable of adequately handling turning, milling, and boring operations. Calibrating a reliable compensation model is a real challenge. Options for reducing modeling and calibration time, an approach to include machine tool multi-functionality in the model structure, model transferability between different machines of the same type, and model verification out of the calibration range are discussed in greater detail.

Keywords: thermal error, compensation, accuracy, machine tool, multi-functionality

1. Introduction

The heat generated by moving axes and machining processes creates thermal gradients, which result in thermal elongation and bending of machine tool (MT) elements. This then deteriorates MT accuracy. Thermal errors can be sufficiently reduced through new design concepts (based on structural and material optimization with respect to thermal errors with precise determination of boundary conditions [1]) and/or through temperature control using advanced cooling systems, components, or additional devices [2]. However, both of these approaches have the drawback of introducing significant additional MT costs. Direct compensation methods (employing additional measuring devices and regular measuring cycles [3]) also adequately increase final product accuracy but undesirably prolong machining time. By contrast, indirect (e.g., software; using mathematical models) compensation of thermal errors between the tool center point (TCP) and workpiece position is one of the most widely employed reduction techniques due to its cost effectiveness, ease of application in real time, and minimal need for additional gauges.

Ordinarily, thermal error models are based on measured auxiliary variables [4] (temperature, spindle speed, etc.). Many strategies have been investigated to establish the models [5], e.g., multiple linear regressions [6], artificial neural networks [7], finite element models (or simplified physical models suitable for real time applications [8]), transfer functions (TF) [4, 9, 10], and others.

The main aim of this study is to increase the accuracy of a target machine through software (SW) compensations used in calculating thermally induced displacements between TCP and a workpiece position. Although real-time SW compensation approaches exist for thermal errors, they have numerous serious drawbacks. The majority of these approaches only presume MT thermo-mechanical behavior under similar conditions to calibration measurements [11], steady states [12], or present simulations with little reference to modern trends such as multi-functional variants of MTs [13]. An approach to thermal error modeling of a multi-functional turning-milling center with respect to variation in typical MT configurations (full-fledged turning, milling, and drilling operations) is proposed in this research. Linear and angular thermal errors are considered. The proposed compensation approach employs different variables as system inputs (temperature [14] as well as NC data [4]). In the final part of the research, the developed compensation model is evaluated in terms of calibration effort through application on a different target machine of the same type. In addition, the

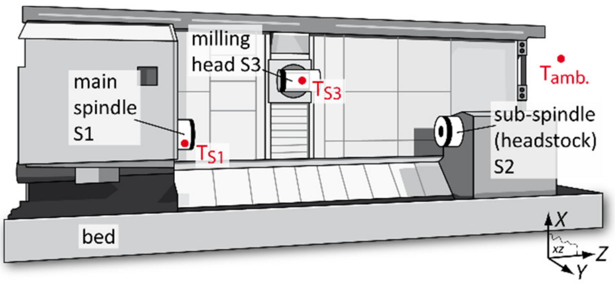

Fig. 1. Schema of the multi-functional turning-milling center.

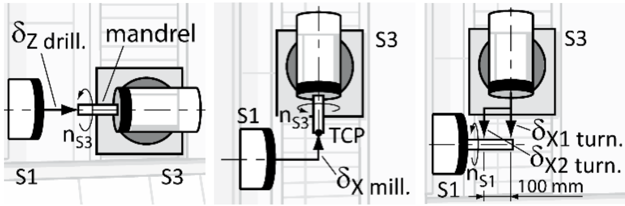

Fig. 2. Typical MT configurations for drilling (left), milling (middle), and turning (right) operations with crucial error directions.

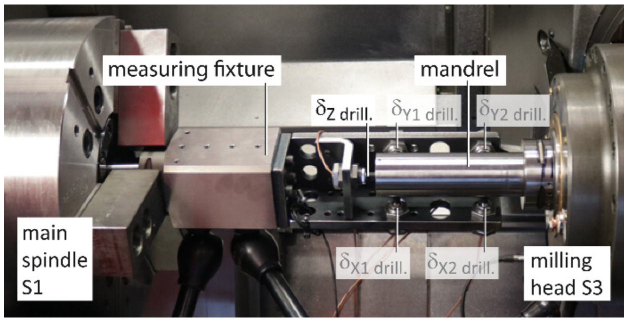

Fig. 3. Experimental setup for drilling configuration.

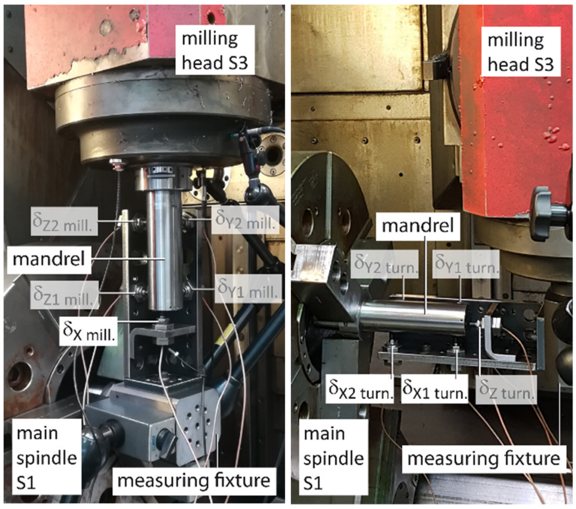

Fig. 4. Experimental setup for milling (left) and turning (right) configurations.

model applicability is verified under different conditions to calibration measurements (different MT axis configurations).

2. Experiment Setup and Conditions

All experiments were performed on a turning-milling center with a maximum turning length of 2,100 mm and maximum turning diameter of 1,150 mm. The maximum main spindle (S1) speed was 2,800 rpm and the maximum milling head spindle (S3) speed was 6,500 rpm. The multifunctional MT is capable of three full-bodied technologies, namely, turning, milling, and drilling. The schema of the examined MT with approximate positions of temperature sensors (used additionally in the modeling part) is shown in **Fig. 1**.

One external RTD sensor (Pt100, Class A, 3850 ppm/K) was used to record ambient temperature changes ($T_{amb.}$ in **Fig. 1**). Eddy current sensors (PR6423, Emerson) firmly clasped in a measuring fixture were used for non-contact sensing of thermal displacements at a micrometer resolution. Relative thermal displacements were measured between the mandrel (length: 125 mm, diameter: 40 mm) representing the TCP and main spindle (regular workpiece position). Other information (spindle bearing temperatures T_{S1}, T_{S3}, and spindle speeds n_{S1}, n_{S3}) was taken directly from the MT control system.

All results and conclusions were closely associated with the following experiment conditions: 1) load-free (without a cutting process); 2) calibration in three MT axis configurations (without any reference to volumetric errors); 3) the compensation model was not implemented into the MT control system and was applied to experimental data offline.

Three experimental setups for typical MT axis configurations corresponding to drilling, milling, and turning operations are schematically depicted in **Fig. 2**.

The situation as depicted in **Fig. 3** describes the real experimental setup of MT axis configurations for drilling operations, where the measuring fixture (representing a workpiece) was mounted on the main spindle, the milling head was equipped with the mandrel (representing a tool), and the milling head was positioned in a horizontal position.

MT axis configurations (along with the real experimental setup) for milling operations are visible on the left side of **Fig. 4**. Similar to the situation shown in **Fig. 3**, the measuring fixture was mounted on the main spindle, and the milling head was equipped with the mandrel. The milling head was positioned vertically in this case.

The right side of **Fig. 4** describes MT axis configurations and the real experimental setup for turning operations, where the measuring fixture (representing a stationary cutter) was mounted on the milling head, the main spindle was equipped with the mandrel (representing a rotating workpiece), and the milling head was positioned vertically.

Linear deformations are dominant when the mandrel is positioned in the milling head (S3), i.e., in milling and drilling configurations. The modeling effort is further focused on deformations in the X (milling) and Z (drilling) directions, as shown in **Fig. 2**.

Changes in diameter are critical during turning operations. The mandrel is short and narrow with respect to the MT working dimensions, and linear deformations related to turning operations are presumably insignificant. By contrast, more significant angular deformations in xz plane were expected. The calculation of the angular component from the measured linear deformations is based on the following equation:

$$\varphi_{xz\ turn.mea.} = (\delta_{X1\ turn.mea.} - \delta_{X2\ turn.mea.}) \cdot 10 \quad . \quad (1)$$

where $\varphi_{xz\ turn.mea.}$ is the angular component of deformation, and $\delta_{X1\ turn.mea.}$ and $\delta_{X2\ turn.mea.}$ are the linear deformations measured during the experiments. The difference in linear deformations was multiplied by 10 to express angular deformations in $\mu\mathrm{m}\cdot\mathrm{m}^{-1}$, as the distance between the measuring positions $X1$ and $X2$ was invariable at 100 mm during all experiments.

3. Calibration, Identification, and Modeling

General demands on a modeling approach of MT thermal errors are based on the use of a minimum of additional gauges to avoid an increase in MT price (using information from the MT control system only if possible), potentialities to real time applications, and ease of implementation into the MT control system. An approach using TFs appears to be a suitable tool to cope with the demands [4, 9, 10].

The compensation strategy based on TFs is a dynamic method with a physical basis. A discrete TF is used to describe the link between the excitation and its response as expressed in the following equation:

$$y(t) = u(t)\cdot\varepsilon + e(t) \quad . \ . \ . \ . \ . \ . \ . \ . \ . \ . \ . \quad (2)$$

where $u(t)$ is the TF input vector in the time domain (temperature or spindle speed), $y(t)$ is the output vector, ε represents the TF in the time domain, and $e(t)$ is the disturbance value (further disregarded).

The different form of the TF in the time domain is introduced by the following equation:

$$\begin{aligned} y(k) = {} & \frac{u(k-i)a_i}{b_0} + \cdots + \frac{u(k-1)a_1}{b_0} \\ & + \frac{u(k)a_0}{b_0} - \left(\frac{y(k-j)b_j}{b_0} + \cdots + \frac{y(k-1)b_1}{b_0}\right) \quad (3) \end{aligned}$$

where $k-i$ ($k-j$) signifies the i-multiple (j-multiple) delay in sampling frequency. Linear parametric models of autoregressive with external input (ARX) or output error (OE) identifying structures were used to set TF calibration coefficients a_i and b_j. The stability of each TF was examined through a linear time invariant (LTI) step response [15]. All data processing, modeling, and simulations were executed in MATLAB and MATLAB SIMULINK software (R2014b).

Analogically to the mechanical TFs, excitations in the employed "thermal" TFs mean that temperatures are measured as close as possible to the described heat sources or the actual spindle speed. The responses represent the linear or angular deflections in the examined directions.

An approximation quality of the simulated behavior is the percentage value (fit) of the output variation reproduced by the model [15]. The fit value given by the following equation is based on the least square method. The 100% refers to the total conjunction of measured and simulated behaviors:

$$fit = \left(1 - \frac{\|\delta_{mea.} - \delta_{sim.}\|}{\|\delta_{mea.} - \bar{\delta}_{mea.}\|}\right)\cdot 100 \quad . \ . \ . \ . \ . \quad (4)$$

where $\delta_{mea.}$ denotes the measured deformation, $\delta_{sim.}$ is the simulated/predicted model output, and $\bar{\delta}_{mea.}$ expresses the arithmetic mean of the measured deformation over time. The vector norm used in Eq. (4) is generally expressed as:

$$\|\delta\| = \sqrt{\delta_1^2 + \delta_2^2 + \cdots + \delta_i^2} \quad . \ . \ . \ . \ . \ . \ . \quad (5)$$

where δ is the general vector of length i.

Because most of the thermo-mechanical process caused by milling head (S3) rotation occurs within the MT component with a small heat transfer to the rest of the MT structure (due to a significant thermal resistance of joint elements between S3 and the rest of the MT), the milling head thermo-mechanical behavior is expected as positionally invariant. For that reason, only one model was developed to approximate both milling and drilling configurations. The model of thermal deformations between the main spindle (S1 – workpiece fixturing) and the milling head (S3 – tool position) is expressed by:

$$\begin{aligned} \delta_{X\ mill.sim.} &= \delta_{Z\ drill.sim.} \\ &= \underbrace{\Delta T_{amb.}\cdot\varepsilon_1}_{ambient} + \underbrace{(\Delta T_{S3} - \Delta T_{amb.})\cdot\varepsilon_2}_{milling\ head\ speed} \quad . \quad (6) \end{aligned}$$

where $\delta_{X\ mill.sim.}$ and $\delta_{Z\ drill.sim.}$ are simulated approximation values, ΔT_{S3} is the milling head bearing temperature expressed in relative coordinates taken directly from the MT control system, $\Delta T_{amb.}$ is information in relative coordinates from the external ambient temperature sensor, and ε_1 and ε_2 are relevant TFs in the time domain. The thermal error model in Eq. (6) is a system that separately resolves the ambient temperature and speed of the milling head impact with subsequent superposition of both elements. The described modeling approach (used also in [4, 9, 14]) generates a transparent model structure, which enables possible description of other thermal sources affecting MT accuracy (feed drives, addition cooling systems, sub-spindle activity, cutting process, etc.).

Angular deformations in the xz plane are dominant during turning configuration measurements. In our study, the main spindle speed was used as system input due to the

Table 1. Setup of calibration tests.

Typical config.	Heat source	Spindle speed [rpm]	Duration [h] Heating	Duration [h] Cooling
Milling	ambient	0	34	
Milling	S3	1400	10	8
Turning	S1	1000	10	10

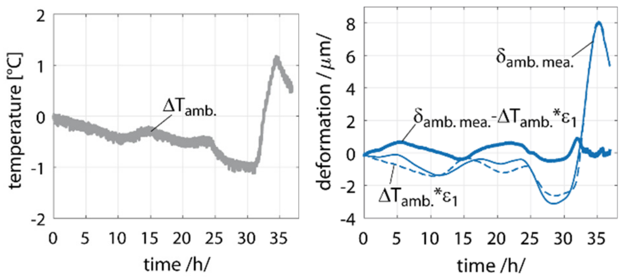

Fig. 5. System input (left) and output (right) during the TF identification process: ETVE test, configuration typical for milling operations.

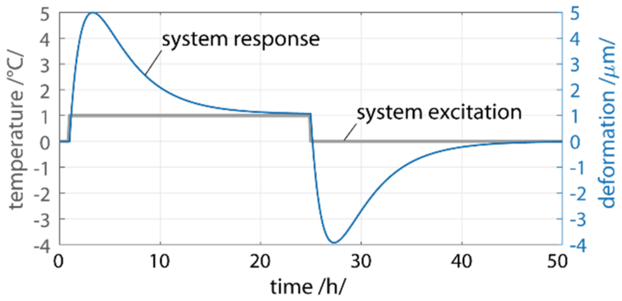

Fig. 6. Stability of the TF (ε_1) identified by the LTI step response.

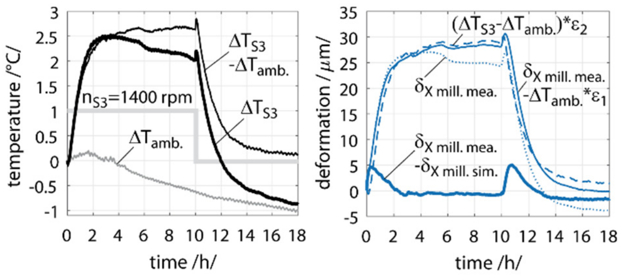

Fig. 7. System input (left) and output (right) during the TF identification process: linear deformations, configuration typical for milling operations.

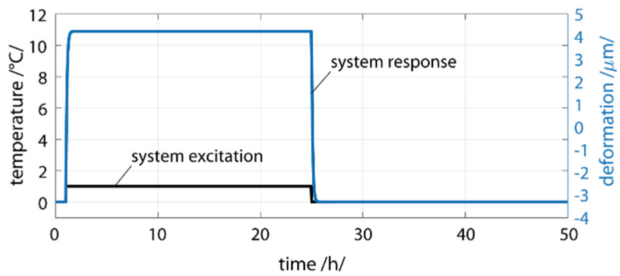

Fig. 8. Stability of the TF (ε_2) identified by the LTI step response.

absence of temperature readings with an obvious correlation to angular deformations. An approximation of angular deformations in the xz plane (the direction from which the tool is applied) is expressed in the following equation:

$$\varphi_{xz\ turn.sim.} = n_{S1} \cdot \gamma_1 \quad \text{. . . . .} \quad (7)$$

where $\varphi_{xz\ turn.sim.}$ is the simulated approximation value, n_{S1} is the actual main spindle speed used as the input value [4], and γ_1 is the relevant TF in the time domain. The influence of the ambient temperature on angular thermal error was not considered.

Three calibration measurements, as summarized in **Table 1**, were necessary to identify model parameters.

Ambient temperature impact on MT accuracy poses a complex issue that requires an autonomous approach [16]. A simplification in terms of only one temperature ($T_{amb.}$) used as a model input parameter is presented in this research. The issue in milling configurations was determined through an environmental temperature variation error (ETVE) test executed based on the international standard ISO 230-3 [17]. Thermo-mechanical system input and outputs along with simulated and residual values during the ETVE test are presented in **Fig. 5**.

The stability of the identified TF ε_1 and a better understanding of the identified ambient temperature thermo-mechanical impact on the examined MT is expressed by an LTI step response (**Fig. 6**), where system excitation represents the sudden change in ambient temperature $\Delta T_{amb.} = 1°$C, and system response is the predicted deformation given by the first part of Eq. (6), namely, $\Delta T_{amb.} * \varepsilon_1$.

The calibration measurements of axes (S1, S3) consist of transient behaviors between two thermodynamic equilibria (MT in approximate balance with its surroundings and MT steady state during heat source activity or during the cooling phase). The TF identification process of milling head activity is shown in **Fig. 7**. The identification process refers to the typical MT configuration for milling operations. The graph on the left side of **Fig. 7** shows inputs into the thermo-mechanical system (the temperature difference $\Delta T_{S3} - \Delta T_{amb.}$), and the graph on the right shows the measured, simulated, and residual outputs. Both phases (heating and cooling) were considered. The ambient temperature impact was extracted from the measured deformations with the help of the first part of Eq. (6) (thin line on the right side of the figure).

The stability of the identified TF ε_2 and a better understanding of milling head activity in the thermo-mechanical behavior of the examined MT is expressed by the LTI step response (**Fig. 8**), where system excitation represents the sudden change of temperature difference $\Delta T_{S3} - \Delta T_{amb.} = 1°$C, and system response is the predicted

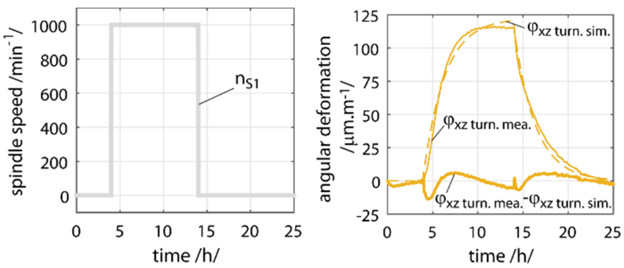

Fig. 9. System input (left) and output (right) during the TF identification process: angular deformations, configuration typical for turning operations.

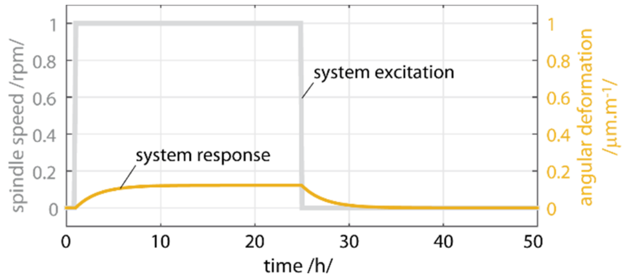

Fig. 10. Stability of the TF (γ_1) identified by the LTI step response.

Table 2. Calibration coefficients of TF model.

TF	a_0 [μm^2/°C]	a_1 [μm^2/°C]	a_2 [μm^2/°C]	b_0 [μm]	b_1 [μm]	b_2 [μm]
ε_1	0.1929	-0.384	0.1912	1	-1.9	0.99
ε_2	0.0642	0	0	1	-0.0025	-0.99
γ_1	0.0063	-0.0126	0.0063	1	-1.9	0.99

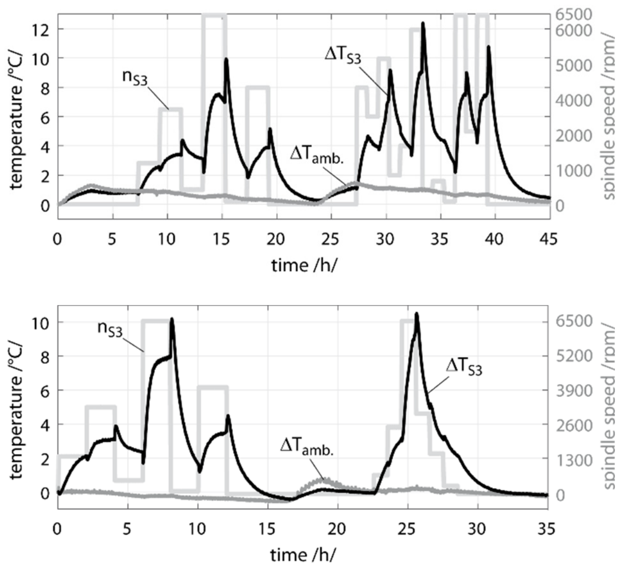

Fig. 11. Compensation model temperature inputs and milling head speed behavior during the milling (upper) and drilling (lower) configuration verification tests.

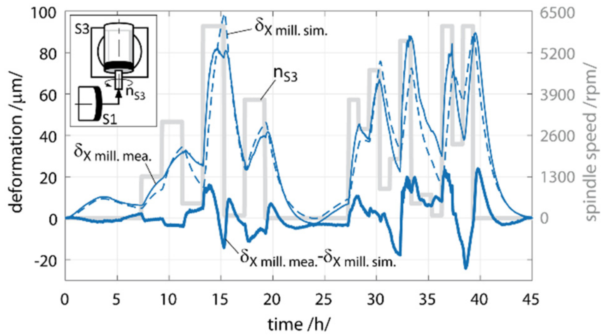

Fig. 12. Application of the TF model to verification experiments of typical configurations for milling operations.

deformation given by the second part of Eq. (6), namely, $(\Delta T_{S3} - \Delta T_{amb.}) * \varepsilon_2$.

The TF identification process of the main spindle activity is shown in **Fig. 9**. The identification process refers to a typical MT configuration for turning operations. The graph on the left side of **Fig. 9** shows input into the thermo-mechanical system (the main spindle speed n_{S1}), and the graph on the right shows the measured, simulated, and residual outputs (angular deformations in xz plain). Both phases (heating and cooling) were considered.

The stability of the identified TF γ_1 and a better understanding of the main spindle activity in the thermo-mechanical behavior of the examined MT is expressed by the LTI step response (**Fig. 10**), where system excitation represents the sudden change in the spindle speed $n_{S1} = 1$ rpm, and system response is the predicted angular deformation given by Eq. (7).

The established calibration coefficients of all identified TFs (see Eqs. (6) and (7)) are summarized in **Table 2**.

The compensation could be realized in a control system through an offsets setup on the MT linear axes. The proposed compensation model has yet to be implemented in an MT control system. All results will be presented as offline applications on measured uncompensated data in the following sections.

4. Application and Verification

Three experiments were conducted to verify the validity of the compensation models. All verification tests consisted of two rpm spectra separated by controlled activity interruption.

The upper part of **Fig. 11** shows thermo-mechanical system temperature inputs during milling configuration verification tests and also shows the milling head spindle speed behavior. The lower part of **Fig. 11** shows the inputs during drilling configuration verification tests and also depicts the milling head spindle speed behavior.

Figure 12 shows outputs (measured thermal errors without compensation) during the milling verification experiment. MT thermal error states after compensation

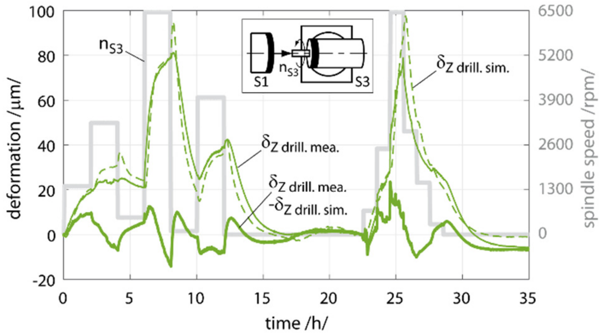

Fig. 13. Application of the TF model to verification experiments of typical configurations for drilling operations.

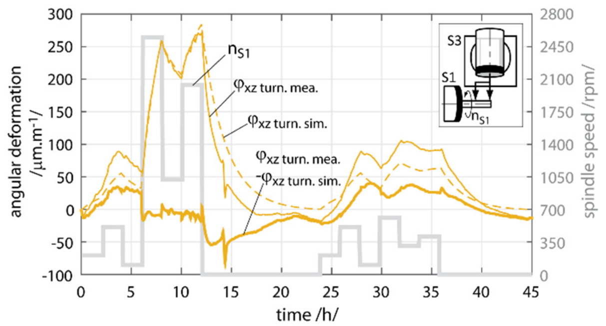

Fig. 14. Application of the TF model to the typical turning operation verification experiment: angular deformations.

were calculated offline based on the difference between the measured and simulated values ($\delta_{mea.} - \delta_{sim.}$). The simulated value ($\delta_{X\ mill.sim}$) was obtained by using Eq. (6).

The improvement of the thermo-mechanical state (expressed by fit; Eq. (4)) was 71% in the milling configuration as compared to the uncompensated state.

Figure 13 shows outputs during the verification experiments with the drilling configuration. The simulated value ($\delta_{Z\ drill.sim}$) was obtained by using Eq. (6).

The improvement of the thermo-mechanical state was 77% in the drilling configuration as compared to the uncompensated state.

Both inputs (main spindle speed) and outputs (measured angular thermal deformations in xz plane) to the thermo-mechanical system during the turning configuration verification test are shown in **Fig. 14**. The calculated residual angular deformations are shown in the same figure (thick line). The simulated value ($\varphi_{xz\ turn.sim.}$; necessary for the residue value calculation) was obtained by applying Eq. (7) to the measured data.

Compared to the uncompensated state, the improvement of the angular thermo-mechanical state in xz plane during the turning configuration was 68%.

A disadvantage of models based on spindle speeds (and other NC data [4, 10]) lies in their indirect connection to a relevant heat source. These types of inputs cannot adequately respond to actual changes in the source (e.g., wear of spindle bearings reflected in increases in temperature).

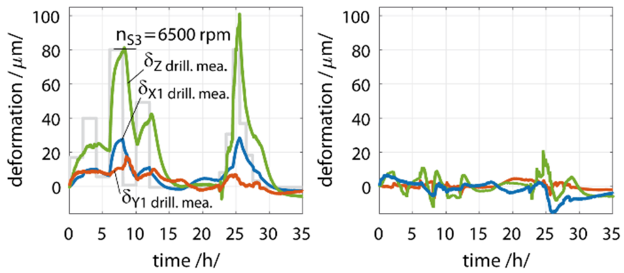

Fig. 15. Comparison of states without (left) and after (right) compensation in X, Y, and Z linear directions: drilling configuration.

5. Discussion

5.1. Compensation Results in Other Directions

Linear thermal error approximations of other directions during drilling (milling) and turning configurations are presented in the following paragraph. A similar structure of thermal error models was applied according to Eq. (6). The identification of TF calibration coefficients approximating the other directions was conducted using the process described in Section 3. All model build-up and identification process details are beyond the scope of this study. For this reason, only short descriptions and results are discussed. The entire data processing and modeling parts of the research lasted up to 40 h.

Models approximating linear deformations of the remaining X and Y directions in the case of the drilling configuration were applied to the verification test from the lower chart in **Fig. 11**. The models had similar temperature inputs to Eq. (6). The measured deformations and results of the models applied in all of the considered directions during the drilling configuration are shown in **Fig. 15**.

The MT accuracy improvements were 10% in the X direction and 74% in the Y direction as compared to the uncompensated state. The symmetrical structure of the milling head resulted in relatively small measured linear deformations in the X direction during the drilling configuration. Compensation of the X direction is possible to neglect for the perspective of the modeling effort and low reduction effect.

Models approximating linear deformations in the X, Y, and Z directions in the case of the turning configuration were applied to the verification test described in **Fig. 14**. A different temperature (main spindle bearings ΔT_{S1} instead of ΔT_{S3}) was used as input along with the ambient temperature $\Delta T_{amb.}$ in the approximation models based on Eq. (6). Temperature inputs during the verification test are shown in **Fig. 16**.

Measured deformations and results of the model applications are shown in **Fig. 17**.

The MT accuracy improvements were 53%, 60%, and 74% in the X, Y, and Z directions, respectively, as compared to the uncompensated state. The most critical deformations in the X direction during the turning config-

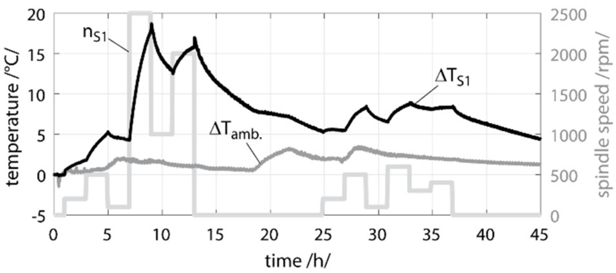

Fig. 16. Model temperature inputs and main spindle speed behavior during the turning configuration verification tests.

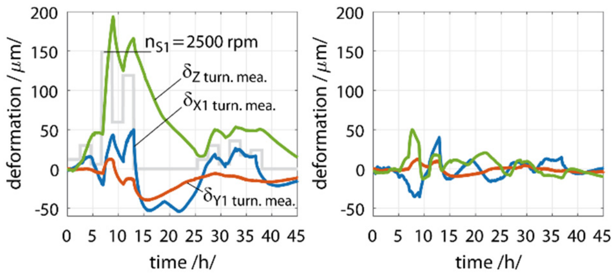

Fig. 17. Comparison of states without (left) and after (right) compensation in X, Y, and Z linear directions: turning configuration.

uration also depend on the workpiece diameter, and this variable should not be overlooked.

5.2. Evaluation of Model Transferability

The industrial applicability of compensation models essentially depends on the calibration effort, specifically, the time to be spent on a new MT to adjust model parameters to enhance MT accuracy to a desired level [10]. Because the compensation model is built up, transferability and adjustment on a different target machine of the same type (the same size and structure) are discussed in further detail.

The setup example for verification experiments on a different target machine corresponds to the left side in **Fig. 4**, that is, the milling configuration. Temperature inputs into the compensation model from Eq. (6) along with the milling head speed spectrum during the verification test are depicted in **Fig. 18**.

Measured deformations and results of the applied thermal error model for the X direction are shown in **Fig. 19**.

The original approximation model from Eq. (6) had to be modified by a coefficient of 0.7 to achieve an 85% thermal error reduction on the examined different target machine for the milling configuration. The thermo-mechanical behavior of the different target machine varied from the original machine in the magnitude of only the approximation value (presumably because of the unknown assembling processes of both spindle heads and different degrees of wear). The time constants of transient thermo-mechanical behaviors of both machines were similar. The correction coefficient 0.7 was sufficient to

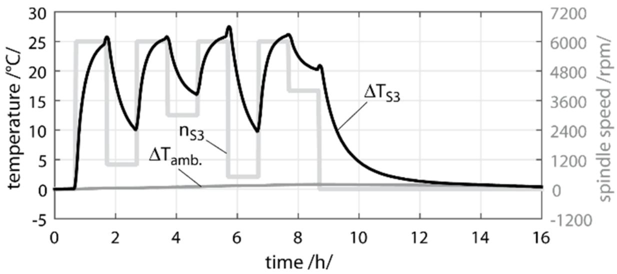

Fig. 18. Temperature inputs and milling head speed behavior during the verification experiment within milling operations: second target machine.

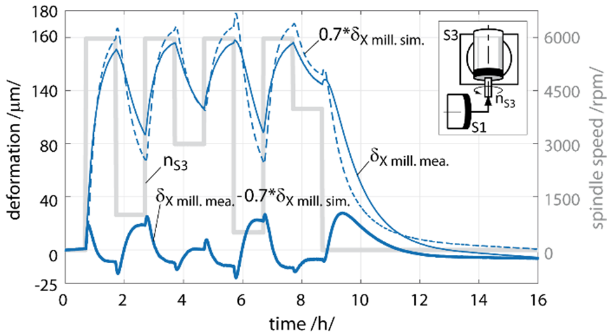

Fig. 19. Application of the TF model to verification experiment within milling operations: second target machine.

achieve a significant thermal error reduction with no need for additional calibration measurements or increase in modeling effort.

The compensation model is sensitive to any changes in thermal sources. The difference in cooling systems or mechanical assembly (including any small alteration in a sub-component supplier) often leads to model failures and recalibration.

5.3. Model Validation Out of Calibration Range

Thermal error compensation models from Eqs. (6) and (7) were calibrated in one MT axis position. A verification test of a model approximating thermal errors induced by milling head activity during the MT milling configuration out of its calibration range was conducted based on the experimental setup shown in **Fig. 20**. The position of the measuring fixture was transferred to the sub-spindle in contrast to its calibration position in the main spindle. The mandrel remained in the milling head, and the milling head was placed in the vertical position, which is a typical configuration for milling operations.

Temperature inputs into the compensation model from Eq. (6) along with the milling head speed spectrum during the verification test are depicted in the upper part of **Fig. 21**. The measured deformations and results of the applied thermal error model for the X direction are shown in the lower part of **Fig. 21**.

The original approximation model from Eq. (6) registered no changes in its structure. The reduction in thermal

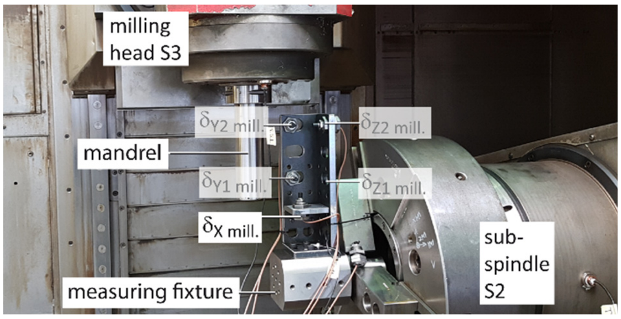

Fig. 20. Experiment MT setup for configurations with measuring fixture clamped in a sub-spindle S2.

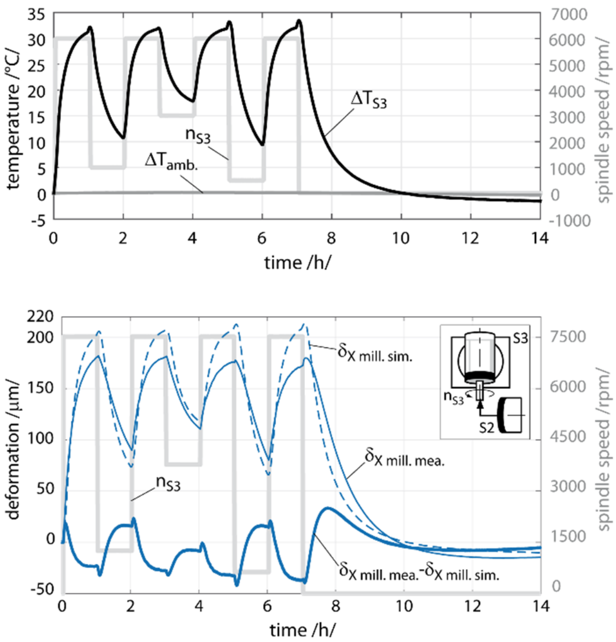

Fig. 21. Temperature inputs and milling head speed behavior (upper) and application of the TF model (lower) to verification experiments of typical configurations for milling operations: setup with sub-spindle S2.

deformations was as much as 80% as compared to the uncompensated state.

Because the model achieved a fine approximation quality through the MT workspace, it should be validated under real cutting process conditions to widen the model's functional guarantee over the calibration range.

6. Conclusion

The main objective of the scientific investigation presented in this study was to enhance MT accuracy by minimizing thermal errors while considering MT multifunctionality. The basic requirements that are typically placed on compensation methods include the role of the main thermal sources, elimination of their influence on various MT configurations, long-term stability, and minimal increase in MT costs. The developed compensation model based on TFs led to promising results, which confirms that TFs are a suitable apparatus for thermal error modeling.

The tested machine was a multifunctional turning-milling center. The experiments were conducted under the following specific conditions: no cutting process was involved and the calibration was performed along the MT axes typical for turning, milling, and drilling configurations. The developed compensation model approximated undesirable thermal errors caused by the main spindle, the milling head spindle rotation, and ambient temperature. Compensation was considered for linear and angular deformation components of thermal errors.

The approximation quality of the models based on TFs was verified during various and long (up to 45 h) main spindle and milling head speed spectra; application on a different target machine of the same type with evaluation of model recalibration effort; and conditions that differed from the calibration tests (model validation through the MT workspace).

A satisfying result of 72% thermal error reduction on average (across all of the presented tests and considered directions) as compared to the original states was achieved.

Follow-up research will focus on testing cutting process impact (at least finishing conditions during milling and turning operations), volumetric accuracy, and thermal error compensation model implementation directly into the MT control system.

References:

[1] J. E. Franke, T. Maier, F. Schäfer, and M. F. Zaeh, "Experimental Evaluation of the Thermal Machine Tool Behavior for Model Updating," Int. J. Automation Technol., Vol.6, No.2, pp. 125-136, 2012.

[2] T. Nozaki and J. Otsuka, "Reduction of Thermal Deformation in a Motor Precision Positioning Device Cooled by Peltier Elements," Int. J. Automation Technol., Vol.7, No.5, pp. 544-549, 2013.

[3] C. Hong and S. Ibaraki, "Observation of Thermal Influence on Error Motions of Rotary Axes on a Five-Axis Machine Tool by Static R-Test," Int. J. Automation Technol., Vol.6, No.2, pp. 196-204, 2012.

[4] C. Brecher and P. Hirsch, "Compensation of thermo-elastic machine tool deformation based on control internal data," CIRP Annals – Man. Tech., Vol.53, No.1, pp. 299-304, 2004.

[5] J. Mayr, J. Jedrzejewski, E. Uhlmann, M. A. Donmez, W. Knapp, F. Härtig, K. Wendt, T. Moriwaki, P. Shore, R. Schmitt, C. Brecher, T. Würz, and K. Wegener, "Thermal issues in machine tools," CIRP Annals – Man. Tech., Vol.61, No.2, pp. 771-791, 2012.

[6] S. R. Postlethwaite, J. P. Allen, and D. G. Ford, "The use of thermal imaging, temperature and distortion models for machine tool thermal error reduction," Proc. Inst. Mech. Eng., Vol.212, No.8, pp. 671-679, 1998.

[7] C. D. Mize and J. C. Ziegert, "Neural network thermal error compensation of a machining center," Prec. Eng., Vol.24, No.4, pp. 338-346, 2000.

[8] M. Gebhardt, A. Schneeberger, S. Weikert, W. Knapp, and K. Wegener, "Thermally Caused Location Errors of Rotary Axes of 5-Axis Machine Tools," Int. J. Automation Technol., Vol.8, No.4, pp. 511-522, 2014.

[9] M. Mareš and O. Horejš, "Modelling of cutting process impact on machine tool thermal behaviour based on experimental data," Procedia CIRP, Vol.58, pp. 152-157, 2017.

[10] C. Brecher and A. Wissmann, "Compensation of Thermo-Dependent Machine Tool Deformations Due to Spindle Load Based on Reduced Modeling Effort," Int. J. Automation Technol., Vol.5, No.5, pp. 679-687, 2011.

[11] S. Xiang, X. Yao, Z. Du, and J. Yang, "Dynamic linearization modeling approach for spindle thermal errors of machine tools," Mechatronics, Vol.53, pp. 215-228, 2018.

[12] S. B. Achour, A. Checchi, G. Bissacco, and L. De Chiffre, "Thermal characterization of a micro polishing machine and effect on path strategy compensation," Proc. of the 19th Int. Conf. and Exhibition (EUSPEN 2019), pp. 446-447, 2019.

[13] T. Moriwaki, "Multi-functional machine tool," CIRP Annals – Man. Tech., Vol.57, No.2, pp. 736-749, 2008.

[14] H. Tachiya, H. Hirata, T. Ueno, Y. Kaneko, K. Nakagaki, and Y. Ishino, "Evaluation of and Compensation for Thermal Deformation in a Compact CNC Lathe," Int. J. Automation Technol., Vol.6, No.2, pp. 137-146, 2012.

[15] L. Ljung, "System Identification Toolbox 7 User's Guide," 2009.

[16] D. Berger, D. Brabandt, and G. Lanza, "Conception of a mobile climate simulation chamber for the investigation of the influences of harsh shop floor conditions on in-process measurement systems in machine tools," Measurement, Vol.74, pp. 233-237, 2015.

[17] Int. Organization for Standardization, ISO 230-3, "Test Code for Machine Tools – Part 3: Determination of Thermal Effects," 2007.

Name:
Martin Mareš

Affiliation:
Research Center of Manufacturing Technology (RCMT), Czech Technical University in Prague (CTU)

Address:
Horská 3, 128 00 Prague 2, Czech Republic

Brief Biographical History:

2008 Received Master degree from CTU in Prague
2015 Received Ph.D. from CTU in Prague
2016- Research Group Leader and Lecturer, Machine Tools Accuracy, RCMT, CTU in Prague

Main Works:

- "Strategy of milling center thermal error compensation using a transfer function model and its validation outside of calibration range," MM Science J., pp. 3156-3163, 2019.
- "Modelling of Cutting Process Impact on Machine Tool Thermal Behaviour Based on Experimental Data," Procedia CIRP, Vol.58, pp. 152-157, 2017.
- "Application of mechatronic approach to modelling, identification and control of machine tool thermal errors," Proc. of the IASTED Int. Conf. on Modelling, Identification and Control, pp. 284-290, 2010.

Membership in Academic Societies:

- European Society for Precision Engineering and Nanotechnology (euspen)
- Association of Engineering Technology (SST)
- Společnost pro Obráběcí Stroje (SpOS)

Name:
Otakar Horejš

Affiliation:
Research Center of Manufacturing Technology (RCMT), Czech Technical University in Prague (CTU)

Address:
Horská 3, 128 00 Prague 2, Czech Republic

Brief Biographical History:

2003 Received Master degree from CTU in Prague
2007 Received Ph.D. from CTU in Prague
2009- Team Leader and Lecturer, Thermal-Mechanical Models, Machine Tools Accuracy, RCMT, CTU in Prague

Main Works:

- "Thermo-Mechanical Model of Ball Screw With Non-Steady Heat Sources," Int. Conf. on Thermal Issues in Emerging Technologies: Theory and Application, pp. 133-137, 2007.
- "Advanced Modelling of Thermally Induced Displacements and Its Implementation into Standard CNC Controller of Horizontal Milling Center," Procedia CIRP, Vol.4, pp. 67-72, 2012.
- "Modelling of Cutting Process Impact on Machine Tool Thermal Behaviour Based on Experimental Data," Procedia CIRP, Vol.58, pp. 152-157, 2017.
- "Thermal errors of a 5-axis CNC milling centre equipped with different spindle units," Euspen's 19th Int. Conf. and Exhibition, pp. 112-115, 2019.

Membership in Academic Societies:

- European Society for Precision Engineering and Nanotechnology (euspen)
- Společnost pro Obráběcí Stroje (SpOS)

Name:
Jan Hornych

Affiliation:
Research Center of Manufacturing Technology (RCMT), Czech Technical University in Prague (CTU)

Address:
Horská 3, 128 00 Prague 2, Czech Republic

Brief Biographical History:

2004 Received Master degree from CTU in Prague
2012 Received Ph.D. from CTU in Prague
2014- Senior Researcher and Lecturer, Metrology Administration Manager of Accredited Testing Laboratory, RCMT, CTU in Prague

Main Works:

- "Advanced thermal error compensation of a flor type machining centre allowing for the influence of interchangeable spindle heads," J. of Machine Engineering, Vol.15, Issue 3, pp. 19-32, 2015.
- "Adaptive Cooling Control of A Ball Screw Feed Drive System," Conf. Proc. Cranfield, Bedfordshire: euspen, Vol.1, pp. 419-422, 2012.
- "Thermomechanical Transfer Functions and Control of a Machine Tool Cooling System," MM (Modern Machinery) Science J., pp. 96-99, 2009.

Membership in Academic Societies:

- European Society for Precision Engineering and Nanotechnology (euspen)
- Společnost pro Obráběcí Stroje (SpOS)